

# A 3-D Interlayer-Based FDTD/NS-FDTD Connection Technique Combined with a Stable Subgrid Model for Low-Cost Simulations

Tadao Ohtani<sup>1</sup>, Yasushi Kanai<sup>2</sup>, and Nikolaos V. Kantartzis<sup>3</sup>

<sup>1</sup>Asahikawa 070-0841, Japan

<sup>2</sup>Niigata Institute of Technology, Kashiwazaki 945-1195, Japan

<sup>3</sup>Aristotle University of Thessaloniki, GR-54124 Thessaloniki, Greece

E-mail: kanai@iie.niit.ac.jp

**Abstract**—An efficient connection scheme for the stable incorporation of several instructive FDTD computing models in the nonstandard (NS)-FDTD method, is proposed in this paper. Based on a straightforward formulation, the novel technique achieves an optimal FDTD/NS-FDTD connection via an interlayer region. Subsequently, the proposed concept is extended to a robust subgrid algorithm for the 3-D NS-FDTD method through the perfectly matched layer condition to decrease the total computational burden. The merits of the combined methodology are numerically validated by diverse applications, such as wire antennas and microwave devices.

**Index Terms**—Antenna radiation patterns, FDTD methods, nonstandard FDTD methods, numerical analysis, subgrids.

## I. INTRODUCTION

The nonstandard (NS)-FDTD method is a time-domain technique for fixed-frequency electromagnetic problems [1], with an error at least 4 orders of magnitude lower than conventional FDTD techniques [2]. To achieve such high accuracy the NS-FDTD method needs about 36 nodes to update each field quantity. If cost-effective computing schemes originally developed for the FDTD algorithm, e.g. the antenna feed model or the contour-path model, were able to be used with the NS-FDTD method, its applicable range would be greatly expanded. This is the objective of this work.

In order to smoothly insert the FDTD models mentioned above into the NS-FDTD method, a new, highly stable, 3-D technique which connects the regions of both methods is introduced in this paper. The two regions are joined together through an interlayer, i.e. a NS-FDTD region with  $\alpha_1 = 1$  and  $\alpha_{2,3} = 0$  [1]. Also, to extend this concept, a precise subgrid model is presented to lower the NS-FDTD simulation costs with partially subwavelength structures. In particular, for the consistent connection of elementary cells with different spatial increments (e.g.  $\Delta$  and  $\delta = \Delta/3$ ), the interlayer formulation is blended with the perfectly matched layer (PML) condition [2]-[4]. Thus, any artificial instabilities that could arise from the field interpolations are drastically diminished. A key advantage of the combined method is its simplicity, along with the absence of complex or specialized algorithms. Numerical results for a thin-wire antenna FDTD model and other microwave structures prove the validity of the proposed formulation.

## II. THE 3-D FDTD/NS-FDTD CONNECTION METHOD

Consider the computational domain shown in Fig. 1, which illustrates the novel connection model for the FDTD and NS-FDTD regions, along with the interlayer region for the mitigation of any discontinuities between the two methods.

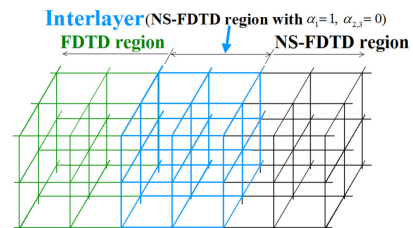


Fig. 1. Lattice topology of the proposed connection model for the FDTD and the NS-FDTD methods through an interlayer region.

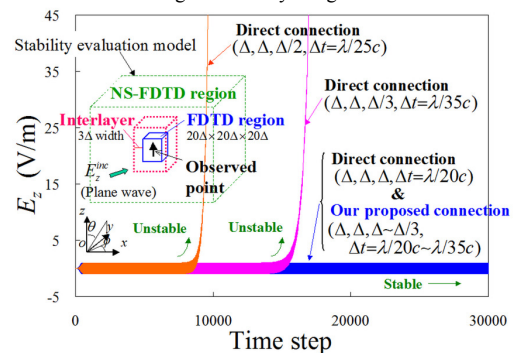


Fig. 2. Stability comparison of the connection model with (proposed) and without (direct) the interlayer region. Incident angle:  $\theta = 90^\circ$  and  $\phi = 10^\circ$ . Fields are observed at the center of the FDTD region ( $|E_z^{inc}| = 1$  V/m).

To stress the necessity of the interlayer region, Fig. 2 provides a stability comparison of our formulation with (proposed) and without (direct) the interlayer for a  $20\Delta \times 20\Delta \times 20\Delta$  FDTD volume embedded in a sufficiently large NS-FDTD domain. The interlayer has a  $3\Delta$  width ( $\Delta = \lambda/10$ ), where  $\lambda$  is the wavelength. For our discretizations, both cubic ( $\Delta, \Delta, \Delta$ ) and two noncubic ( $\Delta, \Delta, \Delta/2$ ), ( $\Delta, \Delta, \Delta/3$ ) cells are utilized, with  $\Delta t = \lambda/(20c)$ ,  $\lambda/(25c)$ ,  $\lambda/(35c)$  as their respective time-steps and  $c$  the speed of light. In the model a sinusoidal plane wave travels from the NS-FDTD into the FDTD region to excite the domain. In this context Fig. 2 reveals that the direct connection model is stable only for cubic cells and is totally unstable for noncubic cells. In contrast, the proposed model is always very stable, regardless of the cell type; a fact which proves the importance of the interlayer in establishing reliable FDTD/NS-FDTD connections.

## III. DEVELOPMENT OF THE ACCURATE SUBGRID MODEL

To reduce the overall system requirements considerably, the above concept is combined with a precise subgrid model. The connection structure is shown in Fig. 3, where the interlayer is the NS-FDTD region, with  $\alpha_1 = 1$  and  $\alpha_{2,3} = 0$ , and a width of  $3\delta$ . All fields

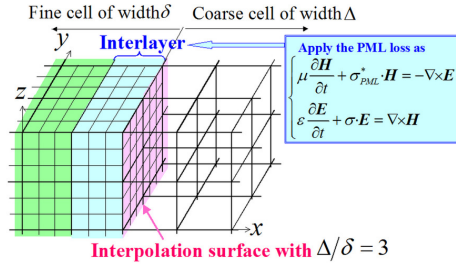


Fig. 3. Geometry of the 3-D connection structure for the subgrid model with the interlayer where a PML condition is imposed for stabilization. All cells are assumed to be cubic and  $E$ -field components are positioned on the grid lines.

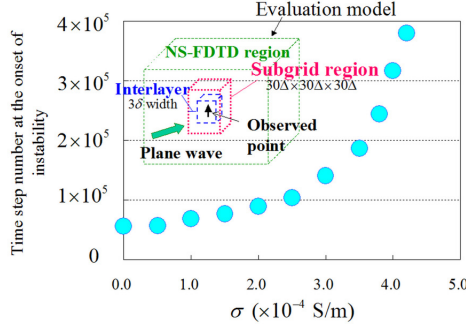


Fig. 4. Effect of PML loss,  $\sigma$ , on the stability of the interlayer-PML. The width of the interlayer is  $3\delta (= \Delta)$ , with  $\lambda/\Delta = 10$ ,  $\Delta t = \lambda/52c$ , and  $\lambda = 1$  m. All fields are observed at the center of the subgrid region.

on the interpolation surface, i.e. the interface between the  $\delta$  and  $\Delta$  cubic cells, are interpolated by a weighted average procedure [2].

Detailed analysis has revealed that, despite the use of this accurate interpolation scheme, instability may arise after a large number of iterations [5]. Hence, to overcome this defect, we impose the PML condition with  $\sigma_{PML}^* = \sigma(\mu/\epsilon)^{1/2}$  to drastically reduce the numerical instability in the interlayer. This is the same approach as in [5], although [5] refers to the case where  $\alpha_{1,2,3} \neq 0$ . To verify this approach, Fig. 4 shows the effect of PML loss,  $\sigma$ , on the performance of our method. A sinusoidal plane wave of  $\lambda=1$  m is launched from the NS-FDTD region (cell size =  $\Delta$ ) into the NS-FDTD subgrid region (cell size =  $\delta$ ). From the results it is easily observed that the interlayer-PML scheme can guarantee a stable subgrid connection over a large number of long time steps. Note that for optimal  $\sigma$  selection, the complexity of the impinging waves [5] must be carefully taken into account.

#### IV. NUMERICAL RESULTS

As an indicative application, we investigate the wire antenna of Fig. 5, which involves a perfect electric conductor (PEC) corner reflector with an angle of  $90^\circ$  [6]–[8]. The radiator, placed along the  $z$ -axis in the FDTD region, forms a  $\phi = 45^\circ$  angle with the  $x$ -axis, while  $S$  is its distance from the corner of the reflector. The feed point is set at the center of the antenna's wire (i.e.  $z=17\Delta/2$ ) to coincide with the reflector's center. Moreover, the input impedance is  $50 \Omega$  and the feed current amplitude is  $1 \text{ A/m}^2$ . For the subgrid region, the cell sizes are  $\Delta=\lambda/22$  and  $\delta=\Delta/3$  respectively, whereas the metallic part uses the contour-path thin-wire FDTD model [2]. Using the connection technique of Section III, the NS-FDTD method is successfully combined with a PML loss of  $\sigma = 5 \times 10^{-4} \text{ S/m}$  for the interlayer. As shown in Fig. 6, the results of the proposed technique are in very good agreement with the reference

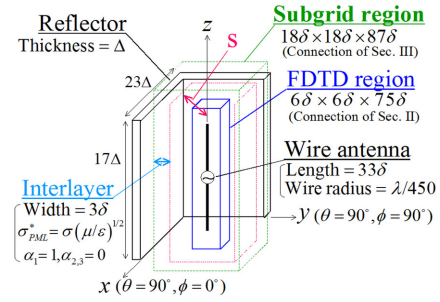


Fig. 5. Wire antenna model [6]. Using the proposed method the total number of cells can be reduced to 1/10 compared with the all- $\delta$ -cell model.

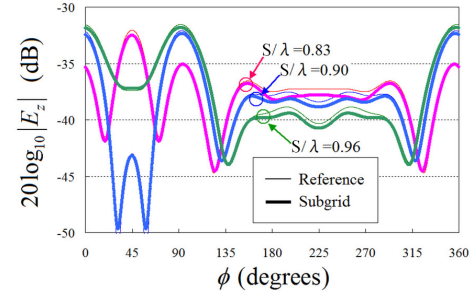


Fig. 6. Far-field radiation pattern on the  $xy$ -plane ( $\theta=90^\circ$ ) for the wire antenna of Fig. 5 ( $\Delta t = \lambda/120c$ , time step =  $2 \times 10^4$ , and  $\lambda = 1$  m).

along the radiation directions of  $0^\circ \leq \phi \leq 90^\circ$  at  $\theta = 90^\circ$ . The reference solution was obtained via the FDTD method [2] with a cubic cell of  $\delta = \lambda/66$ . These results demonstrate the accuracy and stability of our method which, along with its mesh resolution reduction, lead to significant computational savings.

#### V. CONCLUSION

In this paper, a new FDTD/NS-FDTD connection methodology, founded on an interlayer concept, has been developed. The new scheme has also been combined with a 3-D subgrid model for the NS-FDTD algorithm to reduce the computational burden. Numerical simulations have demonstrated the validity of the scheme, thus making it a potential candidate for combining various useful FDTD computing models with the NS-FDTD method.

#### REFERENCES

- [1] J. B. Cole, "High-accuracy Yee algorithm based on nonstandard finite differences: new developments and verifications," *IEEE Trans. Antennas Propag.*, vol. 50, no. 9, pp. 1185–1191, Sep. 2002.
- [2] A. Taflov and S. C. Hagness, 3rd ed., *Computational Electrodynamics: The Finite-Difference Time-Domain Method*. Norwood, MA: Artech House, 2005. Chapters 7, 8, and 10.
- [3] P. Alotto and F. Freschi, "A second-order cell method for Poisson's equation," *IEEE Trans. Magn.*, vol. 47, no. 5, pp. 1430–1433, May 2011.
- [4] V. De Santis, S. Cruciani, M. Feliziani, and M. Okoniewski, "Efficient order approximation for surface impedance boundary conditions in FDTD method," *IEEE Trans. Magn.*, vol. 48, no. 2, pp. 271–274, Feb. 2012.
- [5] T. Ohtani, Y. Kanai, and J. B. Cole, "Stability improvement technique using PML condition for the three-dimensional nonuniform mesh non-standard FDTD method," in *Proc IEEE CEFC 2012*, 2012.
- [6] C. A. Balanis, *Antenna Theory Analysis and Design*. New York, NY: John Wiley & Sons, 2011. Chapter 15.
- [7] P. Scholz, W. Ackermann, T. Weiland, and C. Reinhold, "Antenna modeling for inductive RFID applications using the partial element equivalent circuit method," *IEEE Trans. Magn.*, vol. 46, pp. 2967–2970, Aug. 2010.
- [8] T. Bauernfeind, K. Preis, G. Koczka, S. Maier, and O. Bíró, "Influence of the nonlinear UHF-RFID IC impedance on the backscatter of a T-match tag antenna design," *IEEE Trans. Magn.*, vol. 48, pp. 755–758, Feb. 2012.